

Spatial Coherence Conversion with Surface Plasmons Using a Three-slit Interferometer

Choon How Gan · Greg Gbur

Received: 29 May 2008 / Accepted: 7 August 2008 / Published online: 21 August 2008
© Springer Science + Business Media, LLC 2008

Abstract It has been demonstrated recently that surface plasmons can change the state of coherence of light emanating from a Young's double-slit interferometer. This suggests the possibility of developing a "coherence-converting" device with a large array of subwavelength holes in a metal plate. We have taken an intermediate approach by considering a three-slit geometry, in which we investigated the effects on the modulation of the spatial coherence when an additional slit is placed between the pair of Young's slits. Our results show that the amount of modulation (enhancement or suppression) can be increased or decreased in the three-slit geometry, compared to the double-slit configuration. This is promising for achieving coherence converting optical devices with suitable arrays of subwavelength holes.

Keywords Surface plasmons · Coherence · Subwavelength · Nanotechnologies

Introduction

The ability of a surface plasmon [1] to couple with light and transmit it through subwavelength apertures has made it particularly attractive for deployment in nano-optical devices and systems. Some examples of these include two-dimensional plasmonic optical devices [2, 3], nanoantennas and resonators [4], and super-

resolved optical readout systems [5–7]. In exploring the roles that surface plasmons can play in subwavelength structures, it has recently been shown through a theoretical analysis that surface plasmons can modulate the statistical properties of light in Young's interference experiment [8]. Specifically, it was numerically demonstrated that, depending on the slit separation, the spatial coherence of light emanating from the two slits can be greater or lesser than that of the illuminating field. The spatial coherence of an optical field is a measure of the "statistical similarity" between any two points within the field's domain and its interference-causing capability [9]. The ability of the surface plasmons to enhance the degree of coherence has been demonstrated experimentally in a Young's interferometer, where each slit was separately illuminated by an independent optical source [10]. In that experiment, it was also found that far-field interference fringes are observable even when only a single slit is illuminated. Both observations can be understood by considering that surface plasmons generated at the illuminated slit can propagate to the other slit, where they can couple back into light. This light from the other slit is in turn radiated to the far field, where it interferes with light directly transmitted from the illuminated slit to form fringe patterns.

These results suggest the possibility to change, or even tailor, the degree of coherence of a light field by the use of an array of subwavelength holes in a metal plate. This is important, as the state of coherence of an optical source is a fundamental characteristic that determines numerous properties of the light field it generates, such as its spectrum [11], polarization [12], and directionality [13]. It is not clear, however, if the results for Young's double-slit extend readily to an array of

C. H. Gan (✉) · G. Gbur
Department of Physics and Optical Science, University of
North Carolina at Charlotte, 9201 University City
Boulevard, Charlotte, NC 28223, USA
e-mail: chgan@uncc.edu

holes or slits. This is because the interaction between light and surface plasmons cannot be described accurately through a straightforward superposition of the response from each individual aperture. Thus, it is not known how additional apertures between a given pair of apertures affects the coupling between the original pair, not to mention the effect in the presence of a large array of apertures. Furthermore, unlike the double-slit case where one can examine the coherence properties of light from just two apertures, for an array, one would have to study the coherence properties of light as a global effect resulting from contributions from each aperture in the array.

The aim of this paper is to investigate the coherence properties of light transmitted from a three-slit configuration. We hope to gain an understanding of how the modulation of the degree of coherence changes in the presence of the additional slit. This provides insight to the feasibility of achieving a plasmonic coherence converting device with suitable arrays of subwavelength apertures. Manipulation of the coherence properties may find potential applications in producing coherent light from the spontaneous emission as a result of resonant coupling between semiconductor quantum wells and surface plasmons [14] and in plasmonic interferometry devices, such as all-optical modulators made with quantum dots [15]. In the “Numerical results and analysis” section, results from rigorous numerical simulations are presented, accompanied with discussion and analysis. Following that, we summarize our findings and offer concluding remarks in the “Conclusion” section.

Numerical results and analysis

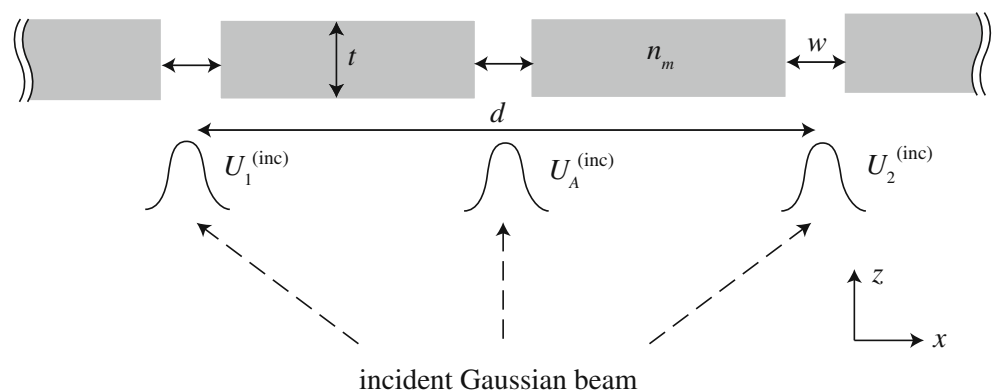
We consider the three-slit geometry depicted in Fig. 1. Each of the slits is illuminated separately with an incident field, which we take to be a quasimonochromatic Gaussian beam synthesized based on the angular

spectrum representation [16, Sec. 5.1]. The beamwidth and wavelength of the incident beam are taken to be 750 and 600 nm, respectively. The incident fields are denoted as $U_1^{(\text{inc})}(\omega)$, $U_2^{(\text{inc})}(\omega)$, and $U_A^{(\text{inc})}(\omega)$, where the subscript A is used to refer to the additional slit in the center and ω is the central frequency of the incident light. The spectral degree of coherence between the incident fields and the fields emerging at any two slits will be denoted, respectively, as $\mu_{ij}^{(\text{inc})}(\omega) = \mu_0(\omega)$, and $\mu_{ij}(\omega)$, where $(i, j = 1, 2, A, i \neq j)$. The metal plate is a gold plate of thickness $t = 200$ nm with three subwavelength slits of width w , and the two end slits separated by a distance d . Its refractive index at 600 nm is taken to be $n_m = 0.21 + i3.27$, after Johnson and Christy [17]. In what follows, we will drop the explicit dependence on ω for brevity.

We have performed rigorous electromagnetic simulations for the three-slit geometry using a Green tensor formalism [18]. Only the case of TM polarization (magnetic field perpendicular to the $x - z$ plane) will be considered since TE-polarized light (electric field perpendicular to the $x - z$ plane) does not excite surface plasmons. We show the simulation results of μ_{12} and μ_{1A} for various values of μ_0 as a function of the slits' separation for slit width $w = 200$ nm in Fig. 2, and for $w = 100$ and 50 nm in Fig. 3. It is observed that, similar to what was found in [8], the degree of coherence μ_{12} and μ_{1A} can be either enhanced or suppressed with respect to the degree of coherence of the incident field μ_0 . Furthermore, the results suggest that μ_{12} and μ_{1A} may be periodically modulated as a function of the slits' separation. Since $\mu_{2A} = \mu_{1A}$ by symmetry, simulation results for μ_{2A} will not be shown. To better relate the effects of the surface plasmons to the numerical results, we attempted to fit the results to an analytic model that takes into account the plasmonic contributions to the field radiated at each of the slits.

Different models to account for surface plasmon generation and plasmon-assisted transmission through

Fig. 1 Depicting the three-slit geometry in consideration



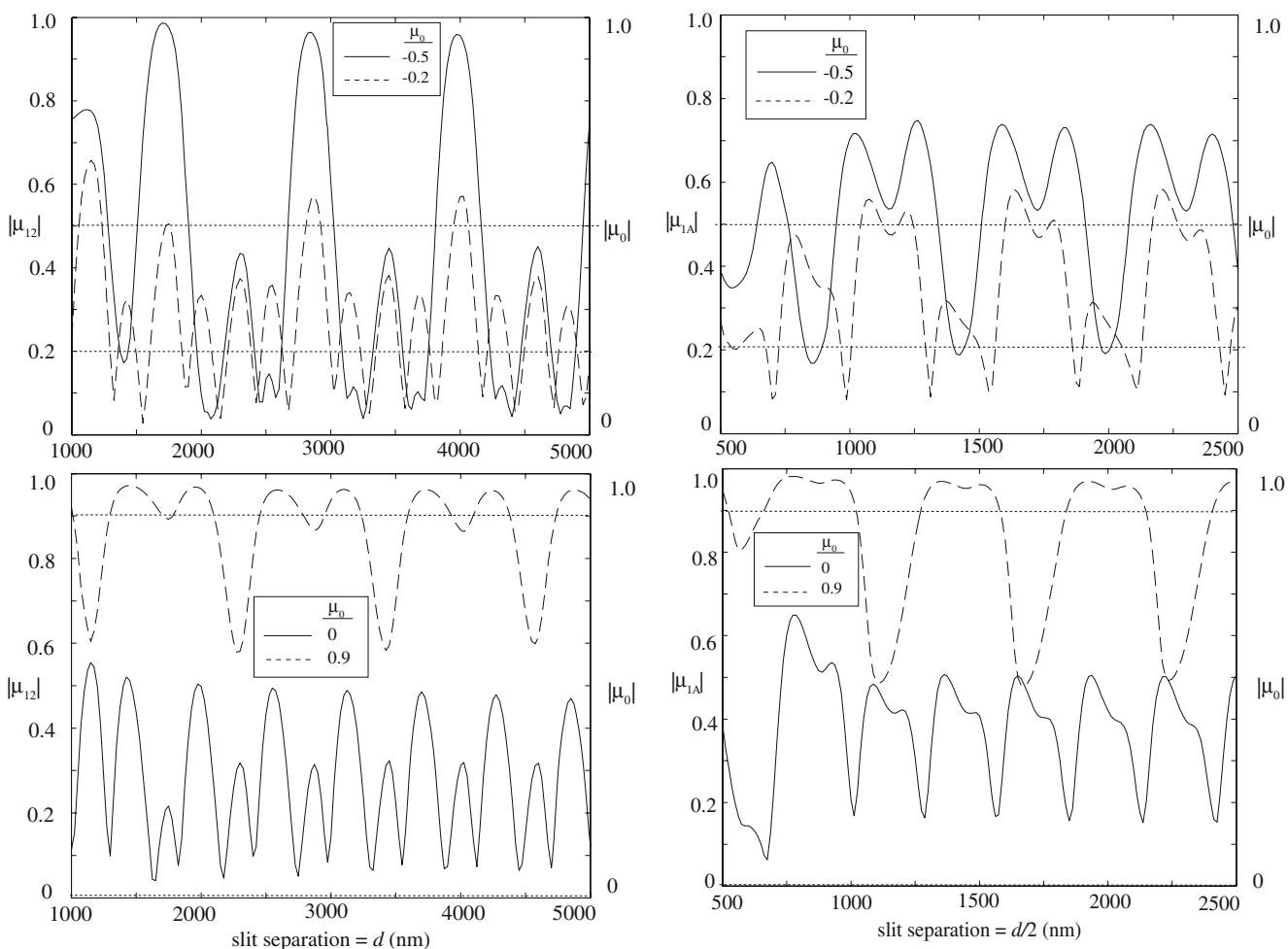


Fig. 2 Simulation results for μ_{12} (left column) and μ_{1A} (right column) for $w = 200$ nm, with different values of the spectral degree of coherence of the incident field μ_0 . Top row: $\mu_0 = -0.5$

(solid line), and -0.2 (dashed line). Bottom row: $\mu_0 = 0$ (solid line), and 0.9 (dashed line). Dotted horizontal lines indicate the respective values of $|\mu_0|$

subwavelength apertures have been proposed by several authors [19–22]. Here, we adopt a model that was used first to explain the enhanced and suppressed transmission due to the effects of surface plasmons propagating between a pair of Young’s double slits [23]. In essence, we have extended the model used in [8] for two slits to include a third slit. At each of the slits, a fraction α of the incident field will be directly transmitted. Part of the incident field will be converted into surface plasmons, which can travel to another slit, whereby the following two situations may take place: (1) part of the plasmonic field couples back to light and reappears as a freely propagating field, and/or (2) part of the plasmonic field is scattered, after which it continues propagating to the next slit, where it couples back to light and reappears as a freely propagating field. These interactions are indicated with the colored arrows in Fig. 4, with the solid, dashed, and dotted arrows representing the contributions to the fields U_1 , U_2 , and

U_A , respectively. The fields U_1 , U_2 , and U_A represent the x component of the electric field, which is the dominant radiating field component. Let us also define the parameter β , which describes the strength of the light-plasmon coupling at each of the slits, and η and Γ , which describe the forward and backward scattering of the plasmonic field by the slits, respectively. The parameters α , β , η , and Γ are complex quantities in general. While α and β are related to three-dimensional propagating fields, η and Γ describe the transmission and reflection of the plasmonic field propagating along the surface of the metal plate. In terms of these parameters and the incident fields, the field at each of the three slits is

$$U_1 = \alpha U_1^{(inc)} + \alpha\beta\eta U_2^{(inc)} e^{ik_{sp}d} + \alpha\beta U_A^{(inc)} e^{ik_{sp}d/2}, \quad (1a)$$

$$U_2 = \alpha\beta\eta U_1^{(inc)} e^{ik_{sp}d} + \alpha U_2^{(inc)} + \alpha\beta U_A^{(inc)} e^{ik_{sp}d/2}, \quad (1b)$$

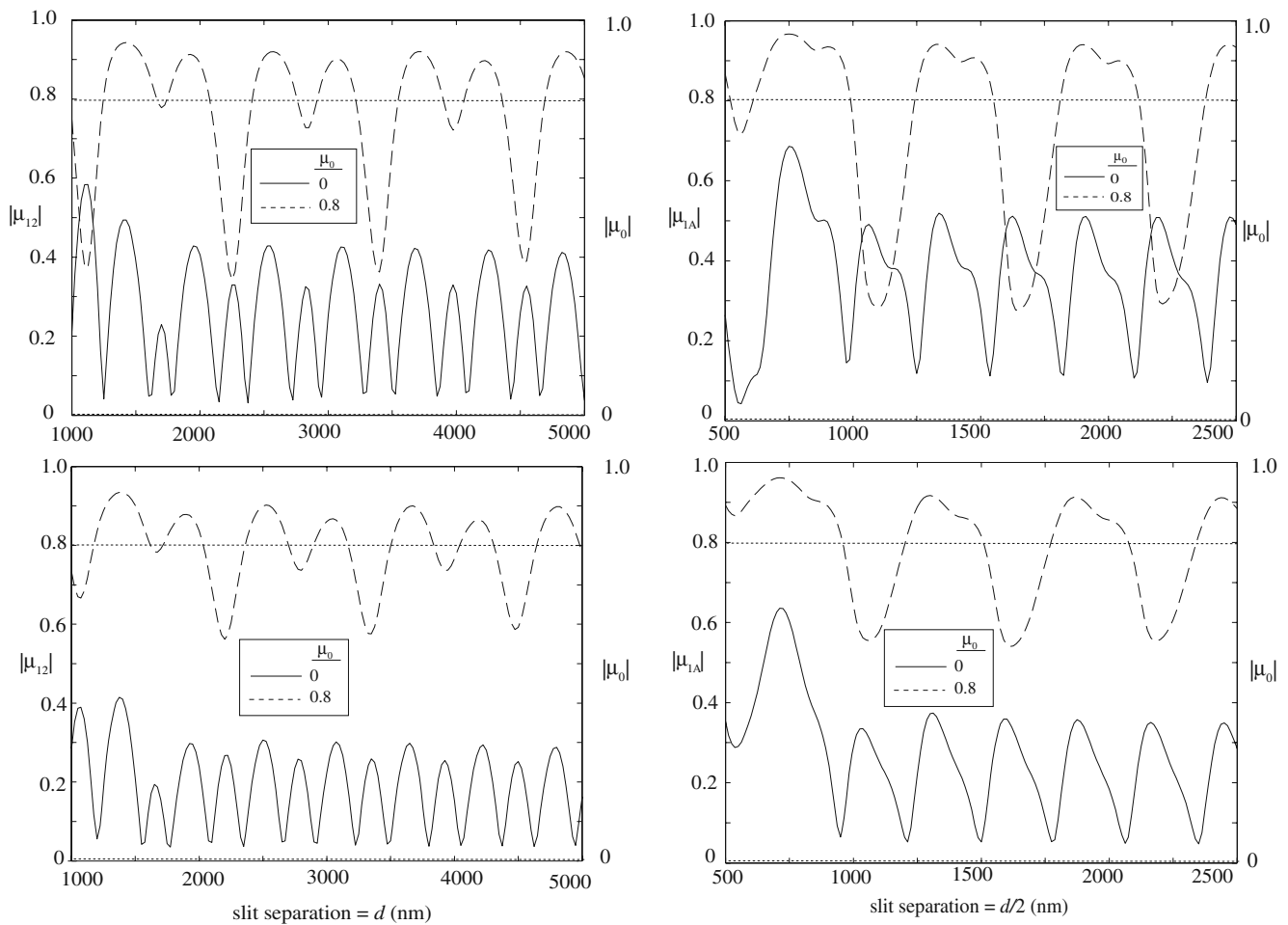


Fig. 3 Simulation results for μ_{12} (left column) and μ_{1A} (right column) for $w = 100$ nm (top) and $w = 50$ nm (bottom). The spectral degree of coherence of the incident field $\mu_0 = 0$ (solid

line) and 0.8 (dashed line). Dotted horizontal lines indicate the respective values of $|\mu_0|$

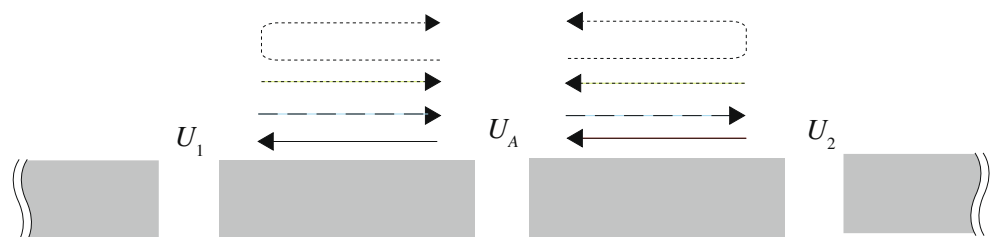
$$U_A = \alpha\beta U_1^{(inc)} e^{ik_{sp}d/2} + \alpha\beta U_2^{(inc)} e^{ik_{sp}d/2} + \alpha U_A^{(inc)} [1 + 2\beta\Gamma e^{ik_{sp}d}], \tag{1c}$$

where k_{sp} is the wavenumber associated with the surface plasmons and d is the distance between slits 1 and 2. The field U_1 at slit 1 in Eq. 1a, for instance, consists of three parts: (1) a directly transmitted part (α); (2) a part that couples to the plasmons at slit 2 (β), “jumps” over the center slit A (η), and coupled to the output (α); and (3) a part that couples to the plasmons at slit

A (β), and coupled to the output (α). It is to be noted that the contribution from surface plasmons that travel from slit 1(2) to slit A , and then are reflected back to slit 1(2), can be expressed as a direct contribution from $U_1^{(inc)}$ ($U_2^{(inc)}$) and may be taken into account by the parameter α in our model. The second-order coherence properties of the fields between any two of the slits may be described by the cross-spectral density function [24]

$$W_{ij} = \langle U_i^* U_j \rangle, \tag{2}$$

Fig. 4 Illustrating the plasmonic contributions to the field radiated at each of the slits considered in our model. The solid, dashed, and dotted arrows represent the contributions to the fields U_1 , U_2 , and U_A , respectively



where the asterisk indicates complex conjugation and angular brackets denote ensemble averaging. As expressed in Eq. 1, each of the fields U_i or U_j in Eq. 2 is a function of the incident fields at the three slits. Using a 3×3 matrix \mathbf{M} to describe the degree of coherence between the incident fields, we can write Eq. 2 in matrix form such that

$$W_{ij} = U^{(i)\dagger} M U^{(j)}, \tag{3}$$

with

$$U^{(i)} = \begin{pmatrix} U_{i1} \\ U_{i2} \\ U_{iA} \end{pmatrix}. \tag{4}$$

Here, the \dagger indicates complex conjugate transpose, and the components of the vector $U^{(i)}$, namely, U_{i1}, U_{i2}, U_{iA} , denote, respectively, the contribution from the incident fields $U_1^{(inc)}, U_2^{(inc)}$, and $U_A^{(inc)}$ to the field U_i as expressed in Eq. 1. The matrix \mathbf{M} takes on the form

$$\mathbf{M} = \begin{bmatrix} 1 & \mu_{12}^{(inc)} & \mu_{1A}^{(inc)} \\ \mu_{21}^{(inc)} & 1 & \mu_{2A}^{(inc)} \\ \mu_{A1}^{(inc)} & \mu_{A2}^{(inc)} & 1 \end{bmatrix}. \tag{5}$$

Since we have assumed that $\mu_{ij}^{(inc)} = \mu_0$, the matrix \mathbf{M} reduces to

$$\mathbf{M} = \begin{bmatrix} 1 & \mu_0^* & \mu_0^* \\ \mu_0 & 1 & \mu_0^* \\ \mu_0 & \mu_0 & 1 \end{bmatrix}, \tag{6}$$

where we have made use of the fact that $\mu_{ij}^{(inc)} = \mu_{ji}^{(inc)*}$. The spectral degree of coherence μ_{ij} of the fields emanating from the slits may then be obtained as

$$\mu_{ij} = \frac{W_{ij}}{\sqrt{S_i S_j}}, \tag{7}$$

where $S_i = W_{ii}$ is the spectral density of the fields at each of the slits. Using Eq. 7, the degree of coherence between any two of the three slits may be calculated. The analytic results were then plotted against the numerical ones, from which it is found that both methods yield values in good agreement. Figure 5 illustrates the agreement between the two sets of results, using the case $w = 100$ nm and $\mu_0 = 0.5$ as an example. Therefore, the model we have developed could be used to analyze the modulation of the degree of coherence as a result of the surface plasmons propagating between the slits. It should be emphasized that the parameters β, η , and Γ in Eq. 1 remain fixed for a given plate index n_m , plate thickness t , and slit width w , independent of the slits' separation or the choice of the two slits for which the degree of coherence is to be calculated.

The analytic results are fitted to the numerical ones for slit width $w = 200, 100$, and 50 nm. The appropriate choices of the values for β, η , and Γ are shown in Table 1. It is worth noting that the values for $|\beta|$, which describes the strength of the light–plasmon coupling, are comparable to those used in [8]. The values of η and Γ did not vary appreciably as the slit width is decreased from 200 to 50 nm. This provides support that η and Γ may be regarded as transmission and reflection coefficients, which should depend largely on

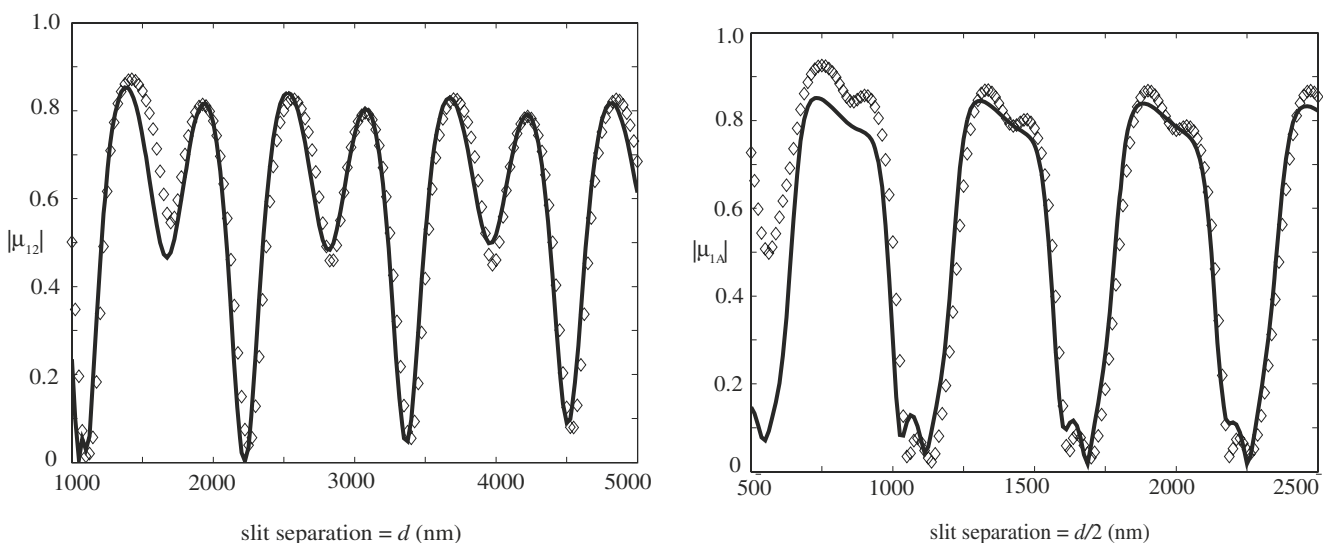


Fig. 5 Simulation results for μ_{12} (left column) and μ_{1A} (right column) for $w = 100$ nm, with spectral degree of coherence of the incident field $\mu_0 = 0.5$. Solid line represents analytic results, and diamond markers represent numeric results

Table 1 Choice of values for the parameters β , η , and Γ for different slit widths (expressed in nanometers)

Slit width (w)	$ \beta $	$\arg(\beta)$	$ \eta $	$\arg(\eta)$	$ \Gamma $	$\arg(\Gamma)$
200	0.33	180°	0.82	0.0°	0.57	230°
100	0.33	190°	0.80	0.0°	0.60	240°
50	0.24	190°	0.78	0.0°	0.60	240°

the refractive index n_m of the metal at each metal/air boundary (assuming the slits are far away enough from each other) rather than on the slit width. It is also found that the choice of a purely real, positive η provides a good fit for both μ_{12} and μ_{1A} , which can exhibit quite different behaviors, as seen in Figs. 2 and 3. Such a real, positive η resembles the forward scattering efficiency in electromagnetic scattering problems [25, Sec. 3.4]. Thus, we could think of η as describing how strongly the slit scatters the plasmonic field in the forward direction.

Finally, we compare the modulation of μ_{12} in the absence and presence of the additional center slit. The results are shown in Fig. 6. It can be seen that, for a given μ_0 , the range of μ_{12} can be larger or smaller in the case of the three-slit geometry. Intuitively, one might expect the additional slit to serve as a barrier for the surface plasmon interactions between the end slits, thus acting to suppress the modulation of μ_{12} , which is indeed the case depicted by the results in Fig. 6. However, the plots also show that there are some instances, for example, with $\mu_0 = -0.5$ and $d \sim 1,700$ nm, where the modulation of the degree of coherence is enhanced in

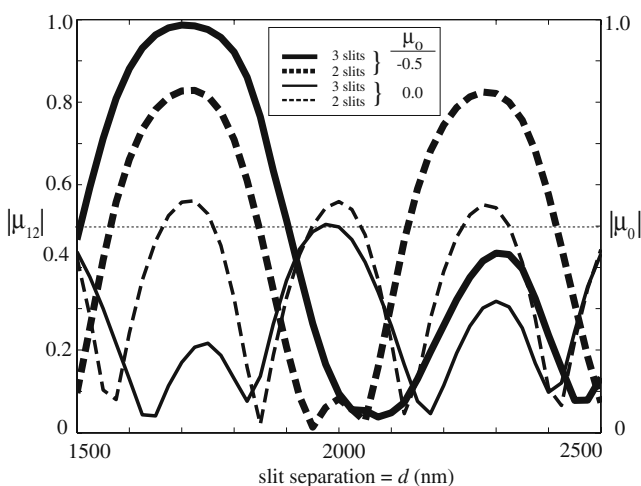


Fig. 6 Comparison of the modulation of the degree of coherence in the presence and absence of the additional slit. The slit width $w = 200$ nm. *Solid lines* represent results with three slits, and *dashed lines* represent results with the *double slits*. The spectral degree of coherence of the incident field $\mu_0 = -0.5$ (*thick lines*) and 0 (*thin lines*). *Dotted horizontal lines* indicate the respective values of $|\mu_0|$

the three-slit geometry. Thus, the additional “barrier” slit can serve not just to decrease the effects of surface plasmons propagating from one slit to the other, but also to preserve, and even enhance, these effects. From these observations, it can be inferred that the additional center slit can either enhance or suppress the modulation of the coherence properties of the fields emanating from the two end slits. This is promising for the development of coherence converting devices with hole arrays in metal plates.

Conclusion

In conclusion, we have shown, using analytic and numerical modeling, that placing an additional slit in between the pair of slits in a Young’s experiment supporting plasmons can either increase or decrease the degree of modulation of the spatial coherence of the fields radiated. While we have restricted our focus to subwavelength slits in the present investigation, it is worthwhile noting that the transport mechanism responsible for optical transmission through subwavelength slits and holes are quite different [26], and therefore, one might expect to observe different behavior between a slit array and a hole array. That the range of modulation of the spatial coherence of the fields radiated from slits 1 and 2 can be increased or decreased in the presence of the additional slit (slit *A*) is an indication that it is indeed possible to develop coherence converting devices with suitable arrays of subwavelength apertures in metal plates. Such coherence converting devices may be very useful in optical systems since the coherence properties of a field strongly affect its propagation characteristics.

Acknowledgement This research was supported by the Department of Energy under Grant No. DE-FG02-06ER46329.

References

1. Raether H (1988) Surface plasmons on smooth and rough surfaces and on gratings. Springer, Berlin
2. Smolyaninov II, Mazzoni DL, Davis CC (1996) Imaging of surface plasmon scattering by lithographically created individual surface defects. *Phys Rev Lett* 77:3877–3880
3. Ditlbacher H, Krenn JR, Schider G, Leitner A, Aussenegg FR (2002) Two-dimensional optics with surface plasmon polaritons. *Appl Phys Lett* 81:1762–1764
4. Bozhevolnyi SI, Søndergaard T (2007) General properties of slow-plasmon resonant nanostructures: nano-antennas and resonators. *Opt Exp* 15:10869–10877
5. Gbur G, Schouten HF, Visser TD (2005) Achieving super-resolution in near-field optical data readout systems using surface plasmons. *Appl Phys Lett* 87:191109

6. Gan CH, Gbur G (2006) Strategies for employing surface plasmons in near-field optical readout systems. *Opt Express* 14:2385–2397
7. Gan CH, Gbur G (2007) Strategies for employing surface plasmons in a near field transmission optical readout system. *Appl Phys Lett* 91:131109
8. Gan CH, Gbur G, Visser TD (2007) Surface plasmons modulate the spatial coherence of light in Young's interference experiment. *Phys Rev Lett* 98:043908
9. Wolf E (2007) Introduction to the theory of coherence and polarization of light. Cambridge University Press, Cambridge
10. Kuzmin N, 't Hooft GW, Eliel ER, Gbur G, Schouten HF, Visser TD (2007) Enhancement of spatial coherence by surface plasmons. *Opt Lett* 32:445–447
11. Wolf E (1986) Invariance of the spectrum of light on propagation. *Phys Rev Lett* 56:1370–1372
12. James DFV (1994) Change of polarization of light beams on propagation in free space. *J Opt Soc Am A* 11:1641–1643
13. Wolf E (1978) Coherence and radiometry. *J Opt Soc Am* 68:6–17
14. Gontijo I, Boroditsky M, Yablonovitch E, Keller S, Mishra UK, DenBaars SP (1999) Coupling of InGaN quantum-well photoluminescence to silver surface plasmons. *Phys Rev B* 60:15564–11567
15. Pacifici D, Lezec HJ, Atwater HA (2007) All-optical modulation by plasmonic excitation of CdSe quantum dots. *Nat Photonics* 1:402–406
16. Stamnes JJ (1986) Waves in focal regions. Adam Hilger, Bristol
17. Johnson PB, Christy RW (1972) Optical constants of the noble metals. *Phys Rev B* 6:4370–4379
18. Visser TD, Blok H, Lenstra D (1999) Theory of polarization-dependent amplification in a slab waveguide with anisotropic gain and losses. *IEEE J Quantum Electron* 35:240–249
19. Genet C, van Exeter MP, Woerdman JP (2005) Huygens description of resonance phenomena in subwavelength hole arrays. *J Opt Soc Am A* 22:998–1002
20. Lalanne P, Hugonin JP, Rodier JC (2006) Approximate model for surface plasmon generation at slit apertures. *J Opt Soc Am A* 23:1608–1615
21. Janssen OTA, Urbach HP, 't Hooft GW (2006) On the phase of plasmons excited by slits in a metal film. *Opt Express* 14:11823–11832
22. Liu H, Lalanne P (2008) Microscopic theory of the extraordinary optical transmission. *Nature* 452:728–731
23. Schouten HF, Kuzmin N, Dubois G, Visser TD, Gbur G, Alkemade PFA, Blok H, 't Hooft GW, Lenstra D, Eliel ER (2005) Plasmon-assisted two-slit transmission: Young's experiment revisited. *Phys Rev Lett* 94:053901
24. Mandel L, Wolf E (1995) Optical coherence and quantum optics. Cambridge University Press, Cambridge
25. Bohren CF, Huffman DR (1983) Absorption and scattering of light by small particles. Wiley, Toronto
26. Barnes WL, Murray WA, Dintinger J, Devaux E, Ebbesen TW (2004) Surface plasmon polaritons and their role in the enhanced transmission of light through periodic arrays of subwavelength holes in a metal film. *Phys Rev Lett* 92:107401